J Mater Sci (2006) 41:7969–7977
DOI 10.1007/s10853-006-0868-z

Electrical and optical properties of $InSbSe_3$ amorphous thin films

M. A. Afifi · E. Abd El-Wahabb · A. E. Bekheet · H. E. Atyia

Received: 28 July 2005 / Accepted: 10 November 2005 / Published online: 7 October 2006

Abstract Electrical conductivity, *I–V* characteristics and optical properties are investigated for $InSbSe_3$ amorphous thin films of different thicknesses prepared by thermal evaporation at room temperature. The composition of both the synthesized material and thin films were checked by energy dispersive X-ray spectroscopy (EDX). X-ray analysis indicated that all samples under investigation have amorphous structure. The dc electrical conductivity was measured in the temperature range (303–393 K) and thickness range (149–691 nm). The activation energy ΔE_σ was found to be independent of film thickness in the investigated range. The obtained *I–V* characteristic curves for the investigated samples are typical for memory switches. The switching voltage increases linearly with film thickness in the range (113–750 nm), while it decreases exponentially with temperature in the range (303–393 K). The switching process can be explained according to an electrothermal process initiated by Joule-heating of the current channel. Measurements of transmittance and reflectance in the spectral range (400–2,500 nm) are used to calculate optical constants (refractive index *n* and absorption index *k*). Both *n* and *k* are practically independent of film thickness in the investigated range (149–691 nm). By analysis of the refractive index *n* the high frequency dielectric constant ε_∞ was determined via two procedures and was found to have the values of 9.3 and 9.15. Beyond the absorption edge, the absorption is due to allowed indirect transitions with energy gap of 1.46 eV independent on film thickness in the investigated range.

M. A. Afifi · E. A. El-Wahabb (✉) · A. E. Bekheet · H. E. Atyia
Physics Department, Faculty of Education, Ain Shams University, Roxy, Cairo, Egypt
e-mail: e_wahabb@hotmail.com

Introduction

Studies of amorphous semiconductors have received much attention because of their interesting electrical, optical and magnetic properties. III–VI semiconducting compounds are useful for many applications in electrochemical devices such as solid solution electrodes. In_2Se_3 is a member of the group of compounds, which are considered as good photovoltaic materials [1]. Several authors have investigated the physical properties of In_2Se_3 [2–4]. Sb_2Se_3 is a V–VI semiconducting compound, which have wide applications in optical and thermoelectric cooling devices owing to its high thermoelectric power and good photoconducting properties. A number of attempts have been made by different workers [5, 6] to investigate its physical properties. The In_2Se_3–Sb_2Se_3 semiconducting compound with very interesting electrical and optical properties is not sufficiently investigated [7, 8].

A few authors have studied the optical [9] and electrical [10, 11] properties of $InSbSe_3$ single crystal. Recently the effect of heat treatment on the structure and the optical properties of $InSbSe_3$ thin films were measured in a small thickness range [12].

The present study aims to investigate the electrical and optical properties of ternary $InSbSe_3$ compound in thin film form with different and wider thickness range.

Experimental techniques

The $InSbSe_3$ compound was prepared in bulk form by the melt-quenching method. A mixture of highly pure components In, Sb and Se of the purity 99.999% in their stoichiometric ratio were weighted and placed in an evacuated silica tube (10^{-5} Torr).The synthesis of the sample was carried in an oscillating furnace to insure the homogeneity of the compound. The temperature of the furnace was raised at a rate of 50 K h^{-1} to 1,003 K [13] and held for 2 days then cooled slowly at a rate of 1 K min^{-1} to room temperature. $InSbSe_3$ thin films with different thicknesses in the range (113–750 nm) were obtained by thermal evaporation of the bulk in a vacuum of 2×10^{-5} Torr and subsequent condensation on highly polished pyrographite and glass substrates kept at room temperature by using Edwards E 306 A coating unit. The film thickness was measured by Tolansky's method of multiple beam Fizeau Frings [14]. The deposition parameters were kept constant for all investigated films. X-ray analysis was used to investigate the structure of the obtained material in bulk and thin film forms whose chemical composition was checked by energy dispersive X-ray analysis (EDX) using JEOL 5400 scanning electron microscope.

Electrical conductivity was studied by measuring the electrical resistance of the investigated films that sandwiched between two Al electrodes using a digital electrometer (Keithley 616). Static *I–V* characteristics were obtained at room temperature as well as at elevated temperatures for thin film samples evaporated on clean highly polished pyrographite substrates using a measuring cell [15]. The potential drop across the studied samples was measured by the above mentioned electrometer. The current passing through the sample was measured by a digital multimeter model TE 924.

The spectral distribution of transmittance *T* and the reflectance *R* for film samples was measured at room temperature using unpolarized light at normal incidence in the wavelength range (400–2,500 nm) with a dual beam spectrophotometer (JASCO Corp., V-750, Rev. 1.00.).

Results and discussion

Structure identification

EDX spectrum analysis showed that the composition of powder and thin film samples are the close in composition to $InSbSe_3$ within an error of ±2% as given in Table 1.

Table 1 Elemental analysis of $InSbSe_3$ (at %)

Element	Bulk	Thin film
In	21.27	20.03
Sb	18.67	17.46
Se	60.06	62.51
Total	100	100

X-ray diffraction patterns for $InSbSe_3$ in powder form, illustrated in Fig. 1 showed its polycrystalline structure. Comparing the obtained lines of the investigated composition with those of its constituent elements Se, Sb and In and the binary compounds In_2Se_3 and Sb_2Se_3 showed the absence of lines of free elements and binary compounds. This comparison indicates that the ternary $InSbSe_3$ polycrystalline compound has been formed.

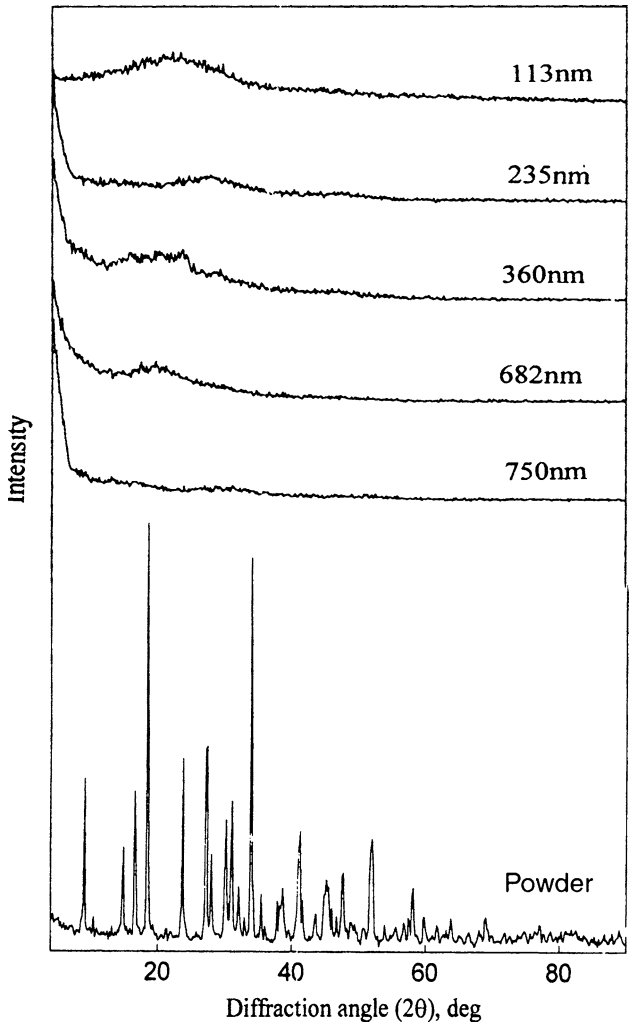

Fig. 1 X-ray diffraction pattern of In Sb Se $_3$ in powder and thin film forms of different thicknesses

X-ray diffraction patterns of $InSbSe_3$ thin films of different thicknesses in the range (149–691 nm), shown also in Fig. 1 indicated their amorphous nature.

Electrical properties

Thickness and temperature dependence of dc conductivity

Thickness dependence of room temperature electrical conductivity (σ) of $InSbSe_3$ thin films was studied in the range (149–691 nm) and is illustrated in Fig. 2a. It is clear that σ increases with increasing film thickness. Such behavior can be attributed to lattice defects such as vacancies, interstitials and dislocations, which developed through the first stage of the film growth during deposition. These defects add an extra one percent to the resistivity. As the film thickness increases, these defects diffuse and, accordingly, the corresponding resistivity decreases and hence the conductivity increases with thickness. It was found that, the room temperature conductivity obtained for $InSbSe_3$ films ($\approx 10^{-8}\ \Omega^{-1}\ m^{-1}$) is less than values obtained earlier [16, 17] ($\approx 10^{-5}$ or $10^{-6}\ \Omega^{-1}\ m^{-1}$) for Sb_2Se_3 films of the same thickness. This explained as: the decrease of Sb atoms in Sb_2Se_3 decreases the free carrier concentration and in turn cause a decrease in the conductivity [18, 19].

The temperature dependence of the electrical conductivity (σ) was studied in the range (303–393 K) and illustrated as $\ln \sigma$ versus $1{,}000/T$ in Fig. 2b. The obtained relation suggests that there is one type of conduction mechanism, which contributes to the conductivity in the considered range of temperature. Also, it indicates that $\sigma(T)$ exhibits activated temperature dependence according to the following relation:

$$\sigma = \sigma_o \exp(-\Delta E_\sigma / k_B T) \quad (1)$$

σ_o is the pre-exponential factor, k_B is the Boltzmann constant, T is the absolute temperature and ΔE_σ is the electrical conduction activation energy. The calculated values of ΔE_σ according to this equation and Fig. 2 was found to be independent on film thickness in the investigated range and have the mean value (0.108 eV). It is noticed that this obtained value of the activation energy is much smaller than half the value of the optical energy gap (1.46 eV), and comparable with the width of the localized state in the gap region below the conduction band E_e (0.103 eV), reported below (in Section Absorption coefficient and energy gap determination). Thus, electrical conduction in the investigated composition takes place by hopping between theses localized states and the conduction band. This is similar to impurity conduction in polycrystalline semiconductors.

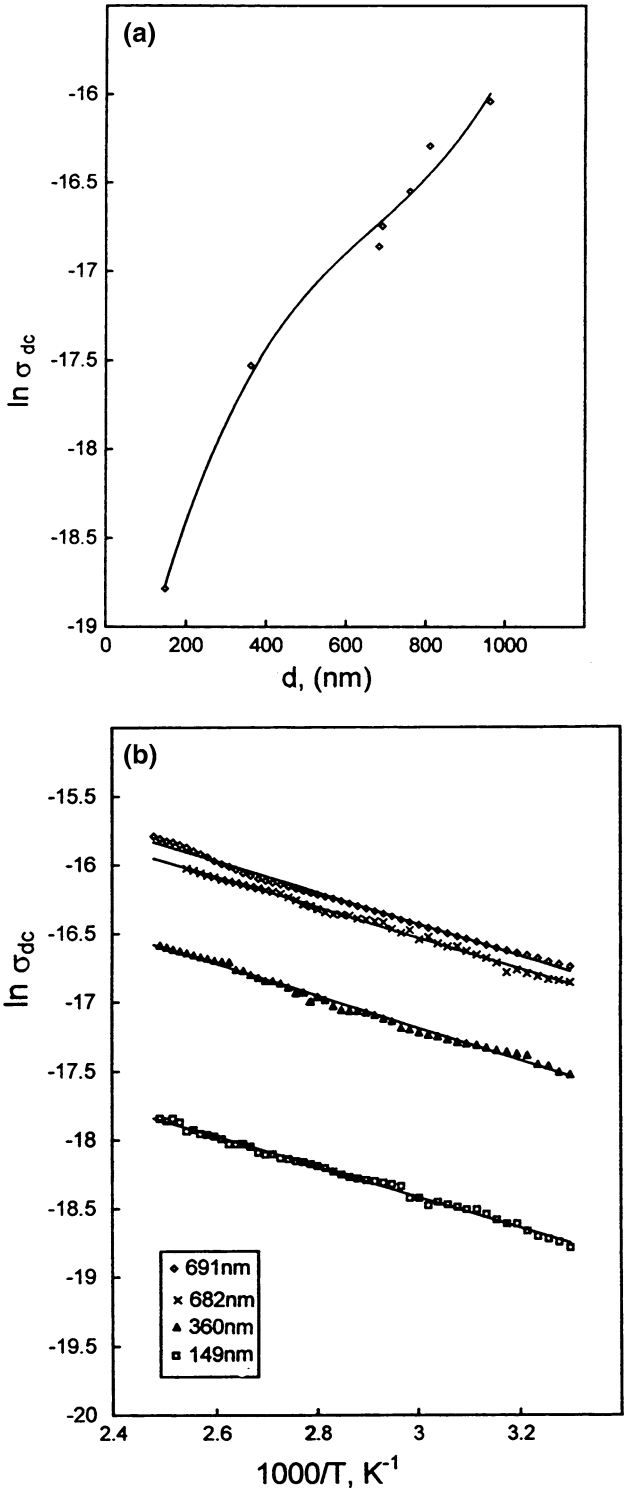

Fig. 2 (**a**) Temperature dependence of dc conductivity σ_{dc} for In Sb Se_3 films of different thicknesses. (**b**) Thickness dependence of room temperature dc conductivity σ_{dc} for $InSbSe_3$ films

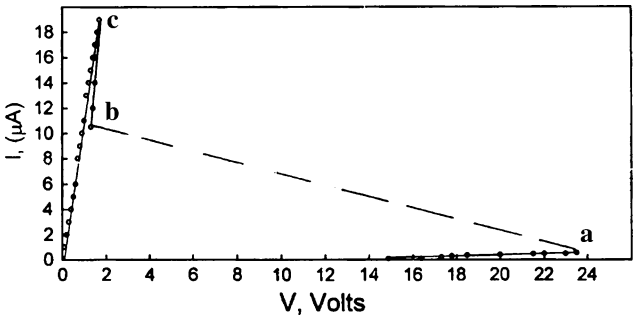

Fig. 3 Static *I–V* characteristic curve for $InSbSe_3$ film of thickness 682 nm

Static and dynamic I–V characteristics

Static and dynamic *I–V* characteristic curves were obtained for $InSbSe_3$ thin films deposited on pyrographite substrates. The obtained *I–V* characteristic curves for films of different thicknesses in the range (113–750 nm) are typical for a memory switch. Figure 3 shows the room temperature static *I–V* characteristic curve for a film of thickness 682 nm as a representative example. It is observed that, when increasing the applied voltage, a small current passes through the samples up to the point a, at which switching takes place. The branch oa represents the OFF-state (with a high resistance). At point a, switching occurs in a very short time (10^{-9} s) i.e., a sudden increase in current and drop in voltage to the point b, therefore, no data points could be taken in this range. A further increase in the applied voltage increases the current without any significant increase in the potential drop "the part bc" forming the ON-state with low resistance. On decreasing the applied voltage in this state, both current and voltage decrease to zero (part co of the curve). If the applied voltage is increased and then decreased, the sample remains in the ON state i.e., the current increased and then decreased along oc and co.

Thickness dependence of switching voltage

Figure 4 illustrates the room temperature *I–V* characteristic curves for $InSbSe_3$ films with different thicknesses in the investigated range (113–750 nm). The threshold voltage was measured for every film sample at different points uniformly distributed throughout the whole surface of the film and their mean value was calculated.

The variation of the mean value of the switching voltage $\overline{Vth}$ with film thickness was studied and displayed in the inset of Fig. 4. A linear relationship between $\overline{Vth}$ and film thickness was obtained in the studied thickness range. The slope of the obtained line represents the mean value of the threshold field $\bar{E}_{th}$ (33×10^6 V/m). The observed relation of thickness dependence of $\overline{Vth}$ agrees with previous observations for different amorphous semiconductor materials [20–22].

Temperature dependence of switching voltage

The temperature dependence of the *I–V* characteristic curves for $InSbSe_3$ thin films was studied in the range (303–373 K) for different thicknesses in the range (113–750 nm). The obtained curves, whose $\overline{Vth}$ values are the corresponding mean values, are shown in Fig. 5 for a film of thickness 237 nm as a representative example. Figure 6a represents the variation of the mean value of the threshold voltage $\overline{Vth}$ with temperature for films with different thicknesses. It is clear that $\overline{Vth}$ decreases exponentially with temperature.

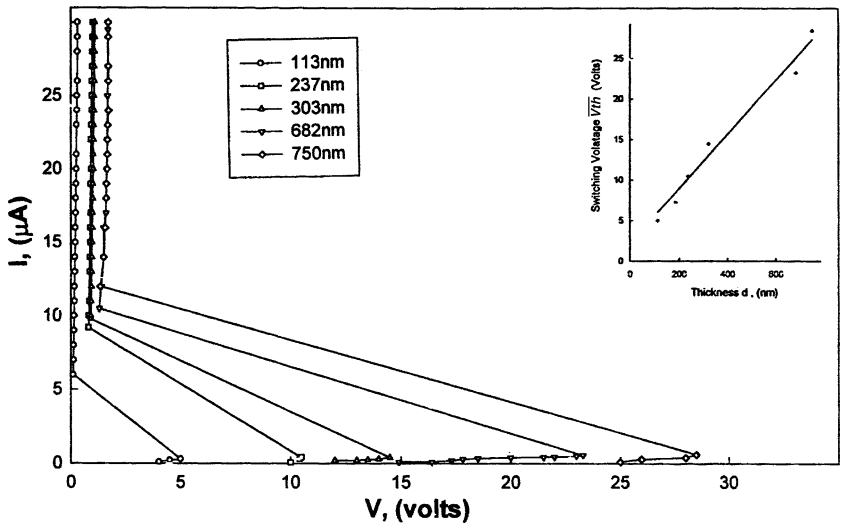

Fig. 4 Static *I–V* characteristic curves for In Sb Se_3 films of different thicknesses and the inset figure shows the thickness dependence of the mean value of the switching voltage $\overline{Vth}$ for In Sb Se_3 films

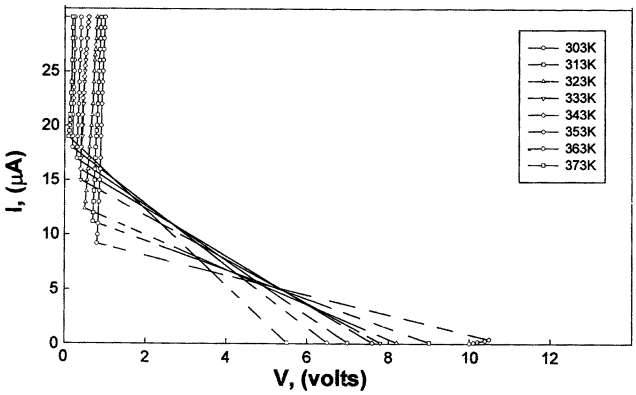

Fig. 5 Static *I–V* characteristic curves for In Sb Se_3 film of thickness 237 nm at different elevated temperatures

The temperature dependence of $\overline{Vth}$ was plotted as ln $\overline{Vth}$ versus 1,000/T for different thicknesses in Fig. 6b. The obtained relation yielded straight lines satisfying the following equation [23]

$$\overline{Vth} = V_o \exp\ (\varepsilon/kT) \tag{2}$$

V_o is a constant and ε is the switching voltage activation energy. The value of ε obtained from the slops of the straight lines of Fig. 6b was found to be independent on the film thickness since the lines are nearly parallel. Its value was found equal to 0.058 eV.

The calculated value of the ratio $\varepsilon/\Delta E_\sigma$ (0.53), agrees with that derived theoretically on the basis of an electrothermal model [15] for the switching process. It agrees also with those values obtained previously [15, 20, 22–27] for other amorphous semiconducting films.

From Eq. 1 and 2 and taking into account that $\varepsilon/\Delta E_\sigma = 0.5$, we obtain the following equation:

$$V_{th}^2/R = \text{constant} \tag{3}$$

This implies that the power dissipated during the switching process is constant. Since, both $\overline{Vth}$ and R are exponentially dependent on temperature, the switching process can be initiated thermally, due to Joule-heating according to an electrothermal model [28, 29] for the pre-switching region.

According to this model, the small difference ΔT between the temperature at the middle of the specimen T_m and that of the surface T_s at the moment of switching is given by the expression [15, 23, 25]:

$$\Delta T_{\text{breakdown}} = T^2/(\Delta E_\sigma/k_B). \tag{4}$$

From this equation and using the value of ΔE_σ, $\Delta T_{\text{breakdown}}$ was calculated for InSbSe3 films at different temperatures and the results are given in Table 2.

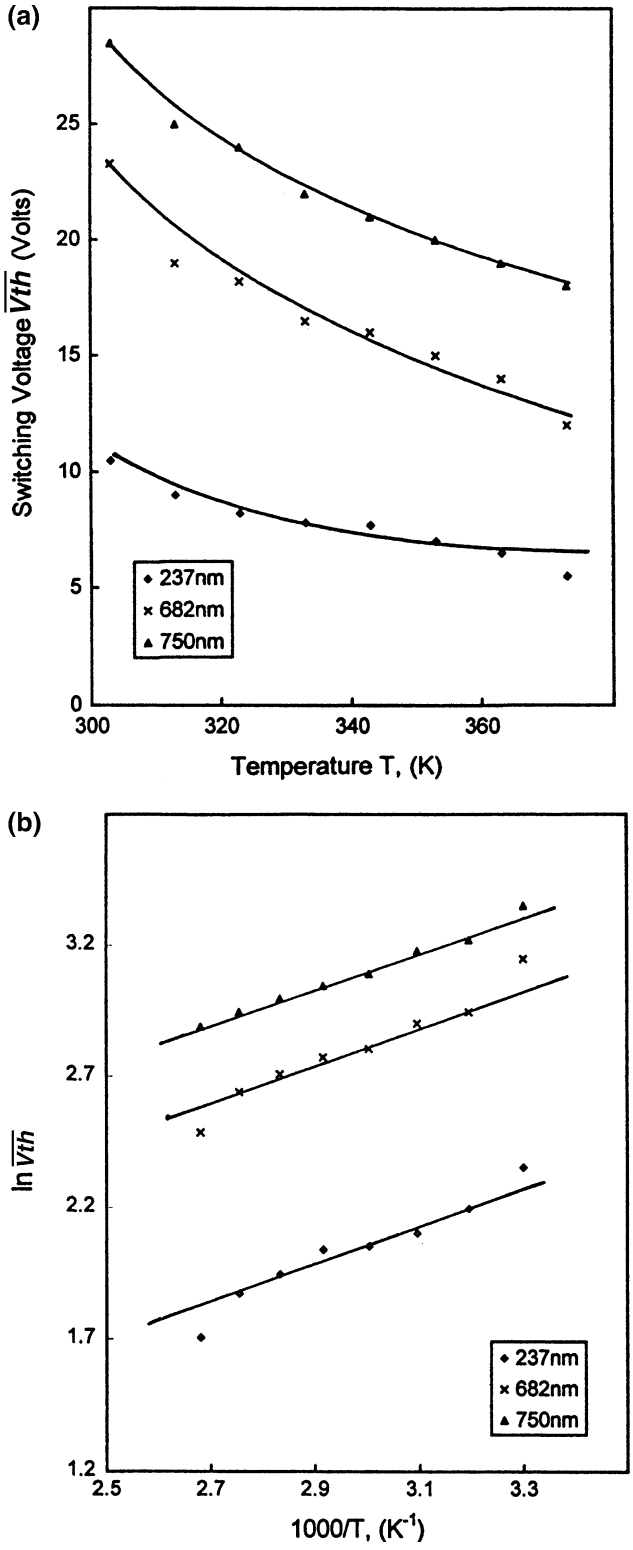

Fig. 6 (**a**) Temperature dependence of $\overline{Vth}$ for $InSbSe_3$ films of different thicknesses. (**b**) The plots of ln $\overline{Vth}$ versus 1,000/T for these films

It is clear that the obtained values are in the same order as the previous results [15, 20, 25, 27] for

Table 2 Values of $\Delta T_{breakdown}$ for InSbSe3 films at different temperatures

T (K)	$\Delta T_{breakdown}$
303	73.31
313	78.24
333	88.55
353	99.51

amorphous semiconducting films. Also, taking into account the good agreement of the obtained value of $\varepsilon/\Delta E_\sigma$ (0.53) mentioned above with both values, the obtained earlier [20, 22–27] and the derived theoretically on the basis of an electrothermal model for switching [15], it can be concluded that the observed memory switching in InSbSe3 films can be satisfactorily explained according to an electrothermal breakdown process.

Optical properties

Determination of optical constants

Figure 7a and b shows the spectral distribution of transmittance T and reflectance R for $InSbSe_3$ amorphous films of different thicknesses in the range (149–682 nm) deposited at room temperature. In order to determine the optical constants (the refractive index n and the absorption index k) for $InSbSe_3$ films, Murmann's exact equations [30] have been applied in conjunction with a special iterative computer program. This method requires approximate values of refractive index n_o and absorption index k_o, which can be obtained using the Swanepoel method [31]. Using the obtained values of n_o and k_o, the accurate values of n and k was calculated.

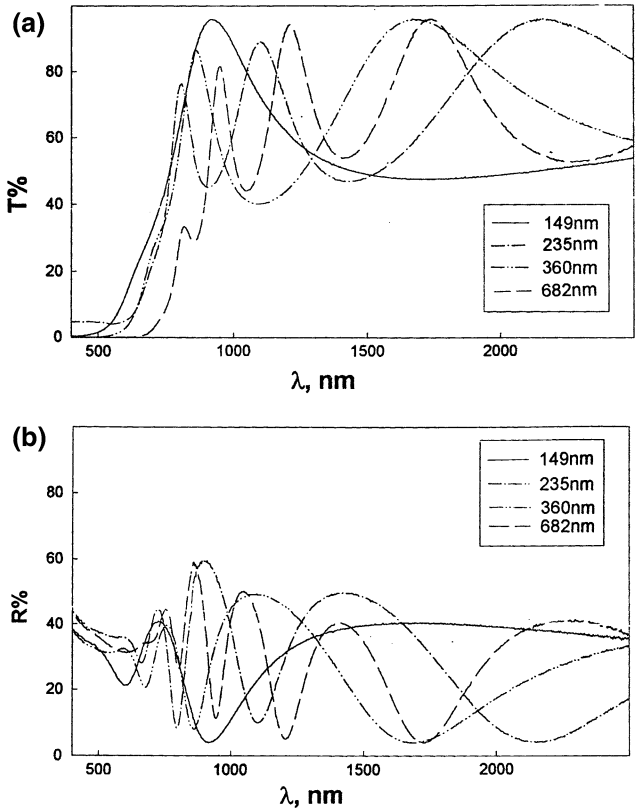

Fig. 7 (**a**) Spectral distribution of transmittance T for In Sb Se_3 films of different thicknesses. (**b**) Spectral distribution of reflectance R for In Sb Se_3 films of different thicknesses

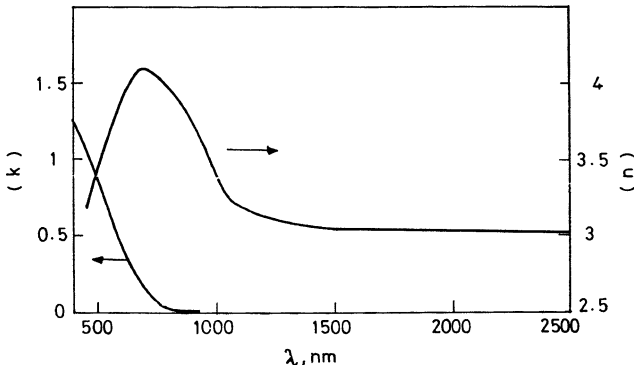

Fig. 8 Dispersion curves of both refractive index n and absorption index k for In Sb Se_3 films

Figure 8 depicts the spectral distribution of both n and k for $InSbSe_3$ thin films of different thicknesses. The discrepancy in the obtained results lies within the range of experimental error of ±6% for n and ±3% for k, accordingly, both n and k are independent of film thickness in the studied range.

Determination of high frequency dielectric constant

The obtained data of refractive index n can be analyzed to obtain the high frequency dielectric constant ε_∞ via two procedures [32]. The first procedure describes the contribution of free carriers on lattice vibrational model dispersion; however, the second procedure is based upon the dispersion arising from the bound carriers in an empty lattice.

In the first procedure n^2 is plotted versus λ^2 as shown in Fig. 9. And the extrapolation of the linear part to zero wavelength gives the value of ε_∞ that was found 9.3.

In the second procedure, at high frequency the properties of $InSbSe_3$ could be treated as that of a single oscillator at wavelength λ_o. The high frequency dielectric constant can be calculated using the following simple classical dispersion relation [32]. If n_o is the refractive index of an empty lattice at infinite wavelength, n will vary as:

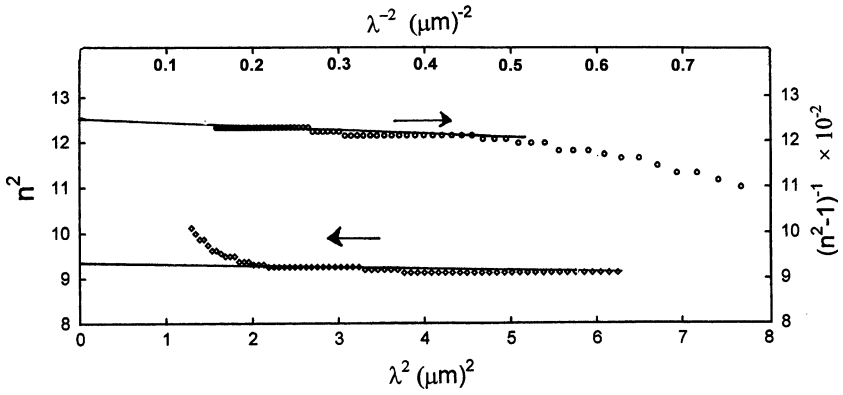

Fig. 9 Plots of n^2 against λ^2 and $(n^2 - 1)^{-1}$ against λ^{-2} for In Sb Se_3 films

$$(n_o^2 - 1)/(n^2 - 1) = 1 - (\lambda_o/\lambda)^2 \quad (5)$$

λ_o and n_o are evaluated from the plot of $(n^2 - 1)^{-1}$ against λ^{-2} shown in Fig. 9. It was found that the value of $\varepsilon_\infty = 9$ since $\varepsilon_\infty = n_o^2$ and $\lambda_o = 270$ nm.

Values of ε_∞, obtained by both procedures are in good agreement with each other within 3.3%. This is because the lattice vibrational and plasma frequencies are well separated from the absorption band-edge frequency.

Equation 5 can also be expressed as [33]:

$$(n_o^2 - 1) = (S_o\lambda_o^2)/[1 - (\lambda_o/\lambda)^2] \quad (6)$$

λ_o is the average oscillator wavelength and $S_o = (n_o^2 - 1)/\lambda_o^2$ is the average oscillator strength which is equal to 11×10^{13} m^{-2} Wemple and Didomenico [34] analyzed the refractive index data below the interband absorption edge using the following single effective oscillator equation

$$(n^2 - 1) = E_d E_s/[E_s^2 - (h\nu)^2] \quad (7)$$

where $h\nu$ is the photon energy, E_s is the single oscillator energy and E_d is the dispersion energy.

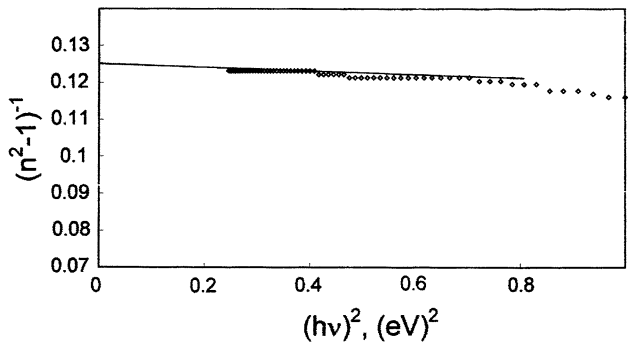

Fig. 10 Plot of $(n^2 - 1)^{-1}$ against $(h\nu)^2$ for In Sb Se_3 films

Values of E_s and E_d were evaluated by plotting $(n^2 - 1)^{-1}$ versus $(h\nu)^2$ and fitting it to a straight line as shown in Fig. 10.

The obtained values of the single oscillator parameters E_s and E_d for $InSbSe_3$ films are 4.6 and 36.88 eV, respectively. The refractive index dispersion parameter E_s/S_o is thus 4.18×10^{-14} eV, which is in the same order of that obtained by Didomenico and Wemple [35] for a number of materials $(6.0 \pm 0.5) \times 10^{-14}$ eV m^2.

Absorption coefficient and energy gap determination

The absorption coefficient α of the investigated films was calculated from the well-known relation $\alpha = 4\pi k/\lambda$ at different values of the wavelength λ in the considered range of spectrum using the corresponding values of k. The obtained values of α as a function of the photon energy $h\nu$ are illustrated in Fig. 11. It is clear

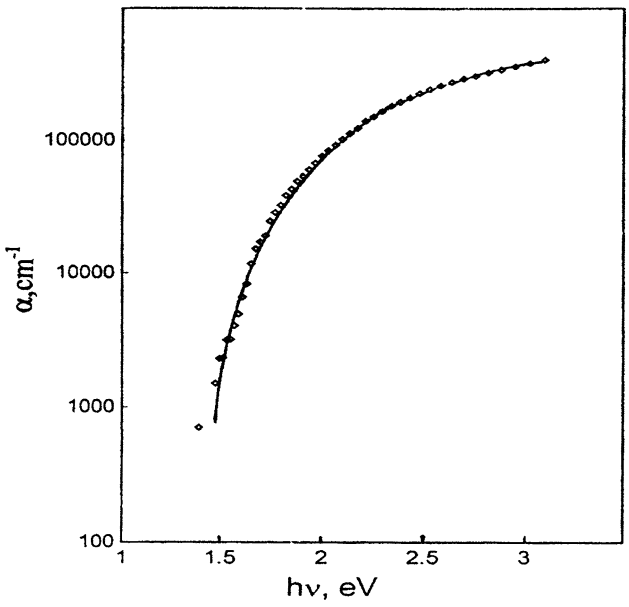

Fig. 11 Optical absorption coefficient α as a function of the photon energy $h\nu$ for In Sb Se_3 films

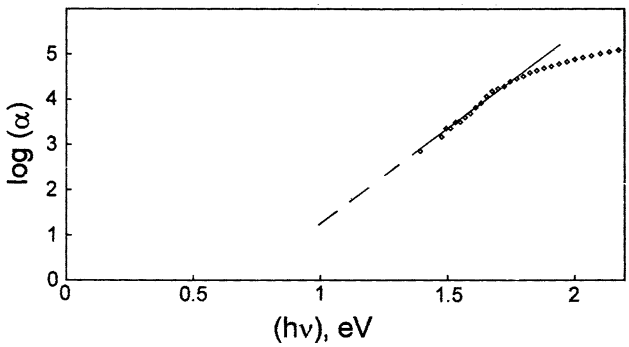

Fig. 12 Plot of log α as a function of the photon energy *hν* for In Sb Se_3 films

from this figure that the spectral distribution of the absorption coefficient can be divided into two regions

(i) For the absorption coefficient $\alpha(\nu) \leq 10^4\ \mathrm{cm}^{-1}$ there is usually an Urbach [36] tail where $\alpha(\nu)$ depends exponentially on the photon energy $h\nu$ as:

$$\alpha(\nu) = \alpha_o\ \mathrm{Exp}\ (h\nu/E_e) \tag{8}$$

ν is the frequency of the radiation, α_o is a constant and E_e is the width of the tails of the localized states at the band gap that represents the degree of disorder in amorphous semiconductors [37]. Valus of α_o and E_e were evaluated from the relation of log α versus $h\nu$ shown in Fig. 12, and were found that ($\alpha_o = 1.26 \times 10^{-3}\ \mathrm{cm}^{-1}$ and $E_e = 0.103$ eV). Accordingly the absorption coefficient of $InSbSe_3$ films in the Urbach tail obeys the relation:

$$\alpha(\nu) = 1.26 \times 10^3 \exp(h\nu/0.103)\ \mathrm{cm}^{-1} \tag{9}$$

(ii) For higher values of the absorption coefficient $\alpha(\nu) > 10^4\ \mathrm{cm}^{-1}$, the variation of the absorption coefficient obeys the relation [38]

$$\alpha(\nu) = A(h\nu - E_g^{opt})^r/h\nu \tag{10}$$

A is a constant, E_g^{opt} is the optical energy gap of the material and r is an index which can be assumed to have values of 1/2, 3/2, 2 and 3 depending on the nature of the electronic transition responsible for the absorption. The usual method for the determination of the value of E_g^{opt} is to plot a graph of $(\alpha h\nu)^{1/r}$ against $h\nu$. Figure 13 shows that the plot of $(\alpha h\nu)^{1/2} = f(h\nu)$ yields a straight line indicating the existence of indirect allowed transitions. Extrapolation of the linear dependence of this relation to the abscissa yields the corresponding forbidden bandwidth E_g^{opt} that was found 1.46 eV. The constant A, determined from the slope of the linear part of this relation is $4.5 \times 10^5\ \mathrm{cm}^{-1}\ \mathrm{eV}^{-1}$. Thus the absorption coefficient in amorphous $InSbSe_3$ thin films obeys the relation

$$\alpha(\nu) = 4.5 \times 10^5 (h\nu - 1.46)^2/h\nu\ \mathrm{cm}^{-1} \tag{11}$$

The optical energy gap for amorphous semiconductors can be determined also from the following equation [39]

$$h^2\nu^2\varepsilon_2 \sim (h\nu - E_g^{opt})^2 \tag{12}$$

ε_2 is the imaginary part of the dielectric constant. The absorption in this region is most easily explained by indirect transitions between the so-called extended states in both valence and conduction bands [39].

Figure 14 shows a plot of $h\nu\sqrt{\varepsilon_2}$ against $h\nu$, which gives a linear part satisfying Eq. 12 for non-direct optical transitions. The extrapolation of this linear part yields $E_g^{opt} = 1.46$ eV. The obtained value of E_g^{opt} from Fig. 14 is in good agreement with that obtained above from Fig. 13.

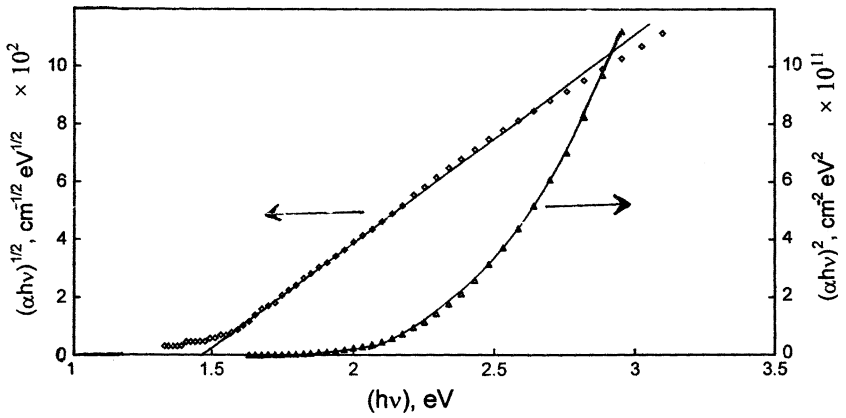

Fig. 13 Dependence of $(\alpha h\nu)^{1/2}$ and $(\alpha h\nu)^2$ on the photon energy $(h\nu)$ for In Sb Se_3 films

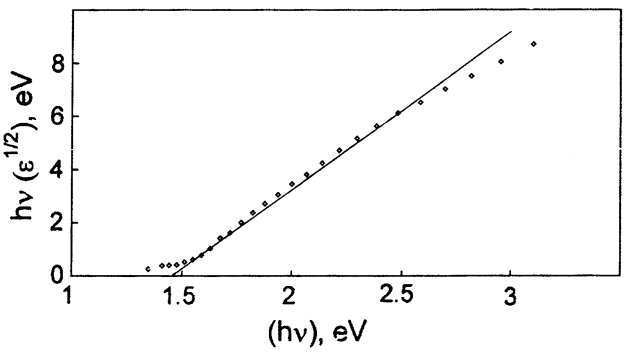

Fig. 14 Dependence of $h\nu\sqrt{\varepsilon_2}$ on the photon energy $h\nu$ for In Sb Se_3 films

Conclusions

The dc electrical conductivity for $InSbSe_3$ amorphous thin films increases with both temperature in the range (303–393 K) and the thickness in the range (149–691 nm). The obtained value of the activation energy ΔE_σ (dc) is found to be 0.108 eV and independent on the film thickness. Static and dynamic *I–V* characteristic curves are typical for a memory switch. The mean value of the threshold voltage increases linearly with film thickness in the range (113–750 nm) and decreases with temperature in the range (303–373 K). The mean calculated value of the ratio $\varepsilon/\Delta E_\sigma$ for $InSbSe_3$ thin films (0.53) agrees with those, the obtained before for different semiconducting compositions and the calculated theoretically on the basis of the electrothermal breakdown process. Values of $\Delta T_{\text{breakdown}}$ calculated on the basis of the electrothermal breakdown process are of the same order as those obtained previously for other chalcogenide glasses. Therefore, the observed memory switching process can be explained according to the electrothermal model.

Optical constants *n*, *k* for $InSbSe_3$ amorphous thin films are determined from transmittance and reflectance measurements in the wavelength range (400–2,500 nm). Both *n* and *k* are found to be practically independent of film thickness in the investigated range (149–691 nm). Analysis of the refractive index *n* by two different procedures yields the high frequency dielectric constant (ε_∞), the average oscillator strength (S_o) and the average oscillator energy (E_s). The analysis of the absorption index indicates that the absorption mechanism is due to indirect transitions with an optical gap of 1.46 eV.

References

1. Herrero J, Ortega J (1987) Solar Energy Mater 16:477
2. Sahu SN (1995) Thin Sol Films 261:98
3. Micocct G, Tepore A, Rella R, Siciliano P (1995) Phys Stat Sol (a) 148:431
4. El-Shair HT, Bekheet AE (1992) J Phys D: Appl Phys 25:1122
5. Abd El-wahabb E, Fouad SS, Fadel M (2003) J Mater Sci 38:527
6. Gilbery LR, Vampelt B, Wood C (1974) J Phys Chem Sol 35:1629
7. Belotskii DP, Babyuk PF, Demyanchuk NV, Noval'Kovskii NP, Bolchuk RF (1970) In: Low temperature thermoelectric materials (in Russion), Kishinev, p 29
8. Wobst M (1967) Z Metallkunde 58:481
9. Gasanly NM, Natig BA, Bakhyshov AE, Shirinov KG (1989) Phys Stat Sol (b) 153:k89
10. Kuliyeva I, Khasanova LKh, Salimova NM (1986) Izv Akad Nauk Azerh SSR Ser Fiz Tekh Mat Nauk (USSR) 5:87
11. Spiesser M, Gruska RP, Subbarao SN, Castro CA, Wold A (1978) J Soli Sta Chem 26:111
12. Soliman HS, Khalifa BA, El-Nahass MM, Ibrahim EM (2004) Physica b 351:11
13. Eddika D, Ramadani A, Brbun G, Tedenac GC, Liautard B (1998) Mat Res Bull 33:519
14. Tolansky S (1984) Multiple beam interferometry of surfaces and films. Oxford University, London and New York, p 147
15. Afifi MA, Hegab NA (1997) Vacuum 48:135
16. Abd El-Salam F, Afifi MA, Abd El-Wahabb E (1993) Vacuum 44:1009
17. Rajpure KY, Lokhande CD, Bhosale CH (1999) Mat Res Rull 34:1079
18. Horak J, Lostak P, Benes LL (1984) Phill Mag B 50:665
19. Lostak P, Navatny R, Kroutil J, Stary Z (1987) Phys Stat Sol (a) 104:841
20. Abd El-Slam F, Afifi MA, Abd El-Wahabb E (1993) Vaccum 44:17
21. Afifi MA, Labib HH, Hegab NA, Fadel M, Bekheet AE (1992) Indian J Pure Appl Phys 30:211
22. Kenawy MA, El-Shazly AE, Afifi MA, Zayed HA, El-Zahid HA (1991) Thin Sol Films, 200:203
23. Mehra R, Shyam R, Mathur PC (1979) J Non-Crys Sol 31:435
24. Bekheet AE (2001) Eur Phus J Appl Phys 16:187
25. Shimakawa K, Inagaki Y, Arizumi T (1973) Jpn J Appl Phys 12:1043
26. Afifi MA, Abdel-Aziz MM, Labib HH, Fadel M, El-Metwally EG (2001) Vacuum 61:45
27. Afifi MA, Labib HH, Hegab NA, Fadel M, Bekheet AE (1995) Indian J Pure Appl Phys 33:129
28. Mehra R, Mathur PC (1979) J Non-Crys Sol 31:435
29. De Wit HJ, Creveccoeur C (1972) Sol State Electron 15:729
30. Murmann M (1933) Z Phys 80:161; (1936) Z Phys 101:643
31. Swanepoel R (1983) J Phys Sci Instrum 16:1214
32. Zemel JN, Jensen JO, Schoolar RB (1965) Phys Rev A 140:330
33. Lee PA, Said G, Davis R, Lim TH (1969) J Phys Chem Sol 30:2719
34. Wemple SH, Didomenico M (1971) J Phys Rev B 3:1338
35. Didomenico M, Wemple SH (1969) J Appl Phys 40:720
36. Urbach F (1953) Phys Rev 92:1324
37. Olley J (1973) Sol State Commun 13:1437
38. Davis EA, Mott NF (1970) Phil Mag 22:903
39. Tauc J, Grigorovic R, Vancu A (1966) Phys Stat Sol B 15:627